

# Super-Poissonian shot noise as a measure of dephasing in closed quantum dots

Daria Dubrovin and Eli Eisenberg

*Raymond and Beverly Sackler School of Physics and Astronomy, Tel-Aviv University, Tel Aviv 69978, Israel*

(Received 20 May 2007; published 28 November 2007)

Electron-electron interactions play a major role in determining the low-temperature rate of phase loss of electrons in mesoscopic systems. The study of the dephasing rate is expected to contribute to the understanding of the many-body nature of such systems. Closed quantum dots are of special interest in this respect, due to theoretical predictions suggesting a possible transition temperature below which the dephasing rate vanishes. This prediction has attracted much attention, since closed quantum dots are prime candidates for storage units in quantum computers, and thus their phase coherence properties are of great importance. However, an effective method for measuring the dephasing rate within a closed quantum dot is still lacking. Here, we study two-level systems and show that the Fano factor has a sharp peak as a function of the chemical potential, the location of which can be simply related to the dephasing rate. We thus suggest to use the properties of the Fano factor peak in the super-Poissonian regime as a probe for the dephasing rate.

DOI: [10.1103/PhysRevB.76.195330](https://doi.org/10.1103/PhysRevB.76.195330)

PACS number(s): 73.63.Kv, 72.70.+m, 73.23.Hk

## I. INTRODUCTION

The study of electrons' phase coherence in mesoscopic systems has been an active field in the past few years. One of the main contributions to the loss of quasiparticle phase coherence (or dephasing) at low temperatures are electron-electron interactions. Thus, measurements of the low temperatures dephasing rate provide us with a valuable probe to gauge our understanding of the structure of the many-electron ground state. In particular, the nature of the many-body wave function in confined geometries was predicted to change sharply at low excitation energies, where the wave function is expected to be localized in Fock space.<sup>1</sup> Consequently, one expects the dephasing rate to vanish at some finite temperature, which scales like  $\Delta\sqrt{g_T}/\ln g_T$ , where  $\Delta$  is the mean-level spacing and  $g_T$  is the dimensionless Thouless conductance of the system. The prediction of vanishing dephasing rate in isolated dots is of great importance in light of the search for systems with long coherence times to be used as storage units in quantum computers. However, it was claimed that the logarithmic correction, and maybe even the existence of the transition are artifacts of various approximations done in the process of mapping the many-body Hamiltonian onto the localization problem.<sup>2</sup> Thus, an experimental verification of this localization transition, through measurements of the dephasing rate in closed (i.e., weakly coupled to the leads) quantum dots, is desirable for both theoretical and applicative reasons.

Whereas there are a number of ways to measure the dephasing times of thermalized states in open quantum dots, the situation is much more complicated in closed dots. Most experiments studying dephasing in closed quantum dots have focused on the relaxation of highly excited states.<sup>3</sup> Some signatures of dephasing in thermalized states were observed in Coulomb blockade conductance maxima<sup>4</sup> and magnetoconductance.<sup>5</sup> The latter was later suggested as a probe for dephasing times in closed dots. Subsequent theoretical analysis<sup>6,7</sup> has yielded some numerical estimates of the dephasing times, and a clear  $\Delta$  dependence was observed. However, it turns out that the magnetoconductance is not

sensitive enough in the low-temperature regime. Although the results of Folk *et al.* are certainly consistent with vanishing dephasing rates at low temperatures, they do not exclude other scenarios.

A renewed interest in charge and current fluctuations and their full counting statistics has arisen recently. These quantities provide additional insight into transport phenomena in mesoscopic systems (see Ref. 8 and references therein). For example, it has been pointed out that the noise of the transferred charge is suppressed in noninteracting conductors and simple quantum dots, as compared to the classical Poisson statistics.<sup>8,9</sup> On the other hand, the shot noise is strongly enhanced in interacting quantum dots.<sup>10-14</sup> The full counting statistics of currents in such mesoscopic systems thus yields a great deal of information on the underlying electronic processes, much beyond what is revealed by the averaged current alone.

In this work, we suggest to use the current fluctuations as a probe of electron dephasing in closed quantum dots. For simplicity, we focus on a two-level model, where dephasing is manifested through the change of the energy state of the dot. We use the noise-to-mean ratio, known as the Fano factor ( $F$ ), as a convenient measure of the shot noise. The classical shot-noise problem, with independent and uncorrelated events, has Poisson statistics, where the Fano factor equals 1. As mentioned above, a single-level quantum dot exhibits suppressed noise, i.e.,  $F < 1$ . The two-level system, on the other hand, may display super-Poissonian noise, due to *dynamical channel blockade*.<sup>15</sup> Here, we examine how this noise enhancement depends on the dephasing rate, i.e., the coupling between the channels.

This paper is organized as follows. In Sec. II we present the model describing the closed two-level quantum dot and arrive at a general expression for the Fano factor. In Sec. III, we proceed to discuss charge transport in the zero bias limit. It is shown that the Fano factor exhibits a sharp peak as a function of the leads' chemical potential, the characteristics of which can be related to the dephasing rate. In Sec. IV, we provide a qualitative description of the random transport process, and in Sec. V, we show that the effect survives ensemble averaging.

## II. FULL COUNTING STATISTICS IN A TWO-LEVEL QUANTUM DOT

We describe the closed quantum dot (QD) as a double-barrier potential well with two energy levels in the transport window ( $\varepsilon_1$  and  $\varepsilon_2$ ), neglecting the influence of all other energy states of the dot. Electrons can transport through the dot by means of tunneling through the barriers. An electron in the excited state, with energy  $\varepsilon_2$ , can decay to the ground state  $\varepsilon_1$  with the rate  $\gamma$ , while an electron in the ground state can be scattered to the excited state with the rate  $\gamma \exp(-\delta/k_B T)$ , where  $\delta = \varepsilon_2 - \varepsilon_1$  is the energy spacing between the two states,  $T$  is the electron temperature, and  $k_B$  is Boltzmann's constant. This relation between the excitation and decay rates is dictated by detailed balance.

The dot is in the Coulomb blockade degenerate regime, where the charge on the dot can fluctuate between  $Ne$  and  $(N+1)e$ . Therefore, the dot can be found in one of three possible states:  $|0\rangle$  where the dot is empty and  $|i\rangle$ , with  $i = 1, 2$ , where one of the two energy levels is occupied. The simultaneous occupation of both energy levels is forbidden

by Coulomb blockade. The transition rates between the occupied states  $|i\rangle$  and the empty state  $|0\rangle$  are  $\Gamma_{i \rightarrow 0} = (1 - f_i^L)\Gamma_i^L + (1 - f_i^R)\Gamma_i^R$  and  $\Gamma_{0 \rightarrow i} = 2f_i^L\Gamma_i^L + 2f_i^R\Gamma_i^R$ , where  $\Gamma_i^\alpha$  is the tunneling rate between the state  $|i\rangle$  and lead  $\alpha$  (left or right),  $f_i^\alpha$  is the Fermi occupation function in the lead,  $f_i^\alpha = 1 / \{1 + \exp[(\varepsilon_i - \mu_\alpha)/kT]\}$ , and  $\mu_\alpha$  is the chemical potential in the lead. The factor 2 accounts for the two spin states in each energy level in the dot.

The Master equation formalism<sup>17</sup> describes the tunneling of electrons through the dot to lowest order in dot-leads coupling (sequential tunneling limit). In order to find the full counting statistics, we follow Bagrets and Nazarov<sup>9</sup> and add counting fields  $\exp(i\chi)$  to the rates involving the change of the dot's excess charge from 0 to  $1e$  ("incoming" events). The cumulant generating function is then proportional to the smallest eigenvalue of the modified rates matrix,  $S(\chi) = -t_0 \Lambda_{\min}(\chi)$ , as long as  $t_0$ , the duration of a single experiment, is longer than the typical dwell time in the dot. The cumulants are given by  $C_n = (-i)^n \partial^n S(\chi) / \partial \chi^n |_{\chi=0}$ . Applying this approach to the general two level case, one obtains the Fano factor

$$F = 1 + 2 \left\{ \frac{\Gamma_{0 \rightarrow 1}\Gamma_{1 \rightarrow 0} + \Gamma_{0 \rightarrow 2}\Gamma_{2 \rightarrow 0}}{\Gamma_{0 \rightarrow 1}\Gamma_{2 \rightarrow 0} + \Gamma_{0 \rightarrow 2}\Gamma_{1 \rightarrow 0} + \Gamma_{1 \rightarrow 0}\Gamma_{2 \rightarrow 0} + \gamma\Gamma_{in}(1 + e^{-\delta/kT}) + \gamma(\Gamma_{1 \rightarrow 0} + e^{-\delta/kT}\Gamma_{2 \rightarrow 0})} - \frac{\Gamma_{in}[\Gamma_{1 \rightarrow 0}\Gamma_{2 \rightarrow 0} + \gamma(\Gamma_{1 \rightarrow 0} + e^{-\delta/kT}\Gamma_{2 \rightarrow 0})][\Gamma_{tot} + \gamma(1 + e^{-\delta/kT})]}{[\Gamma_{0 \rightarrow 1}\Gamma_{2 \rightarrow 0} + \Gamma_{0 \rightarrow 2}\Gamma_{1 \rightarrow 0} + \Gamma_{1 \rightarrow 0}\Gamma_{2 \rightarrow 0} + \gamma\Gamma_{in}(1 + e^{-\delta/kT}) + \gamma(\Gamma_{1 \rightarrow 0} + e^{-\delta/kT}\Gamma_{2 \rightarrow 0})]^2} \right\}, \quad (1)$$

where  $\Gamma_{in} = \Gamma_{0 \rightarrow 1} + \Gamma_{0 \rightarrow 2}$  and  $\Gamma_{tot} = \Gamma_{0 \rightarrow 1} + \Gamma_{1 \rightarrow 0} + \Gamma_{0 \rightarrow 2} + \Gamma_{2 \rightarrow 0}$ . The Fano factor depends on the dephasing rate  $\gamma$ , so in principle it can be used to determine this rate experimentally, provided all the other parameters are known. However, the dependence on the various parameters is much too complex to allow for a practical use of this formula. In the next section, we focus on the zero bias regime and present a setup where the expression for  $F$  can be greatly simplified.

## III. ZERO-BIAS REGIME

Within the zero bias limit, the average current through the dot vanishes. However, transfer of charge between the leads and the island persists. The statistics of this random process can be conveniently studied by examination of those events when electrons enter the dot. The tunneling rates now take the form

$$\begin{aligned} \Gamma_{i \rightarrow 0} &= (1 - f_i)(\Gamma_i^L + \Gamma_i^R) \equiv (1 - f_i)\Gamma_i, \\ \Gamma_{0 \rightarrow i} &= 2f_i(\Gamma_i^L + \Gamma_i^R) \equiv 2f_i\Gamma_i. \end{aligned} \quad (2)$$

Alternatively, one can study the setup where one of the contacts is pinched off, leaving the dot in contact with a single lead, as illustrated in Figs. 3(a) and 3(b).

In Fig. 1, the zero-bias Fano factor (1) is plotted as a function of the chemical potential in the low-temperature

limit,  $k_B T \ll \delta$ . Two distinct regimes are observed. When the chemical potential in the leads  $\mu$  is within the range of  $k_B T$  near the ground level, noise is suppressed below the Poisson value, in agreement with previous observations and predictions in single-level dots.<sup>9,16</sup> In this case the excited level doesn't effect the transport, as its energy is far above the chemical potential. Accordingly, no dephasing effects are observed. However, when both energy levels are below the chemical potential,  $\mu \sim \varepsilon_2$ , and the two transport channels are distinguishable (i.e., the tunneling rates through them are different), the role of dephasing is revealed.

For  $\mu$  in the vicinity of the excited level, strong noise enhancement is observed at low dephasing rates,  $\gamma \ll \Gamma_1$ , and a peak appears in the Fano factor as a function of chemical potential. The height of the peak, as well as its location, clearly depend on the dephasing rate, as seen in Fig. 1(a). As dephasing grows stronger, the noise is suppressed, reaching the limit of  $F \sim 1$  when dephasing rates are high. Strong coupling between the two states causes them to become indistinguishable, so that the system becomes effectively a single energy level. In Fig. 1(b), the role of the ratio between the two tunneling rates  $\Gamma_1$  and  $\Gamma_2$  is demonstrated; the noise enhancement is stronger when the excited level has stronger coupling with the leads. As this coupling becomes weaker, the influence of the second level can be neglected, leading to the Poissonian noise of a single level dot.

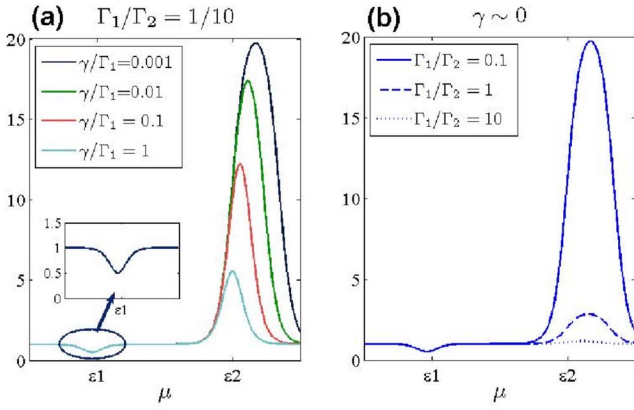


FIG. 1. (Color online) (a) The Fano factor is plotted for several values of dephasing rates at a very low temperature ( $k_B T / \delta = 1/20$ ). In the super-Poissonian region the Fano factor shows a clear peak, the height of which depends on dephasing. Note the shift in the location of the peak with the changing of  $\gamma$ . Inset:  $F$  reaches a minimum value of  $1/2$ , when  $\Gamma_{1 \leftarrow 0} = \Gamma_{0 \leftarrow 1}$ . (b) The Fano factor for various values of the ratio  $\Gamma_1/\Gamma_2$ , and very weak dephasing.  $F$  is dramatically increased when the coupling of the ground level  $\varepsilon_1$  with the lead is considerably weaker than that of the excited level  $\varepsilon_2$ .

Following these findings, we now look for a more convenient expression for the Fano factor, in order to characterize the dependence of the peak's location on the parameter  $\gamma$ . Expanding Eq. (1) to the leading order in  $e^{-\delta/kT}$  in the super-Poissonian regime, where  $\mu \sim \varepsilon_2$ , leads to

$$F = 1 + 2 \frac{\Gamma_{2 \leftarrow 0} \Gamma_{0 \leftarrow 2}}{\Gamma_{1 \leftarrow 0} \Gamma_{0 \leftarrow 2} + \gamma(\Gamma_{1 \leftarrow 0} + \Gamma_{2 \leftarrow 0})}. \quad (3)$$

In order to determine the location of the peak  $\mu_{\max}$ , we use the fact that the Fermi occupation function  $f_1$  is almost constant in the super-Poissonian regime, and so the line shape of  $F$  is determined predominantly by the change of the function  $f_2$ . Using this approximation, one obtains

$$\mu_{\max} - \varepsilon_2 = -\frac{1}{2} k_B T \log \left( \frac{1/\Gamma_1 + 1/\Gamma_2}{1/\gamma + 1/\Gamma_2} \right). \quad (4)$$

When  $(\Gamma_1, \gamma) \ll \Gamma_2$ , a further simplification is possible,

$$\mu_{\max} - \varepsilon_2 = -\frac{1}{2} k_B T \log(\gamma/\Gamma_1). \quad (5)$$

Figure 2 demonstrates the quality of this zero temperature approximation for both the Fano factor and the peak's location. It should be noted that the logarithmic dependence of the peaks' location on  $\gamma$  persists at higher temperatures [Fig. 2(e)], where approximation (3) breaks down.

#### IV. QUALITATIVE DESCRIPTION

The super-Poissonian behavior in the zero-bias regime can be intuitively understood within the dynamical channel blockade picture of Ref. 15. The super-Poissonian statistics is most pronounced at low temperatures, stronger coupling of

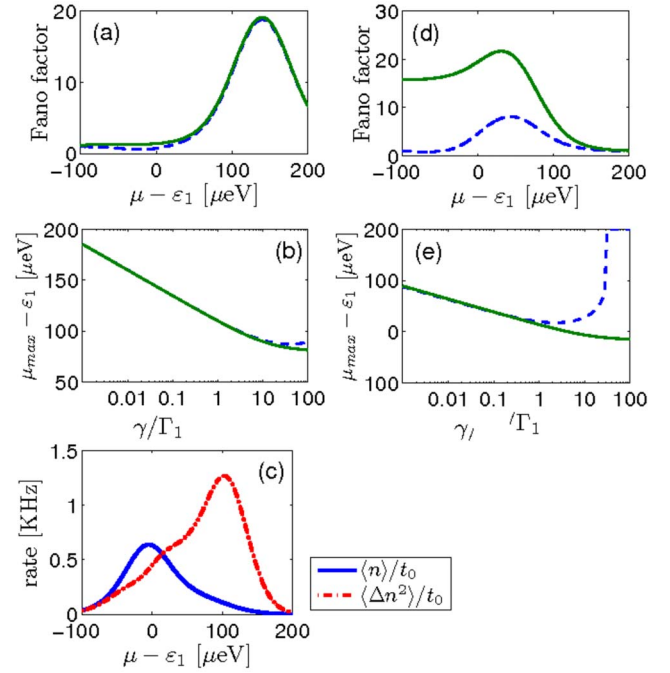


FIG. 2. (Color online) A sample calculation of the cumulants  $C_1$  and  $C_2$  using experimentally relevant parameters (Ref. 12). Tunneling widths are  $\Gamma_1 = 1.6$  kHz and  $\Gamma_2 = 23$  kHz. The electron temperature is  $T_{el} = 230$  mK ( $k_B T \sim 22$   $\mu\text{eV}$ ). Panels (a)–(c) present the low-temperature limit,  $\delta = 5k_B T$ . We set the energy of the lower state  $\varepsilon_1$  as zero, while the excited state has energy  $\varepsilon_2 = 110$   $\mu\text{eV}$ . (a) The Fano factor, evaluated from the general solution [Eq. (1)], compared with the zero temperature approximation [Eq. (3)], dashed and solid lines, respectively. (b) Peak's location for various dephasing rate values. The dashed line was obtained by an explicit calculation of the full expression [Eq. (1)] at different values of  $\gamma$ . The solid line is expression (4). (c) The first two cumulants. For the conditions above and decay rate  $\gamma \sim 0.09$  kHz, the peak is at  $\mu \sim 1.8$   $\mu\text{eV}$ , where the cumulants are  $C_1 \sim 30$  Hz and  $C_2 \sim 600$  Hz. (d) The Fano factor and (e) the location of peak are calculated at a higher temperature to energy spacing ratio,  $\delta \cong 0.63k_B T$  ( $\varepsilon_1 = 0$  and  $\varepsilon_2 = 14$   $\mu\text{eV}$ ). Note the logarithmic behavior of the peak's location.

the excited state to the lead ( $\Gamma_1 \ll \Gamma_2$ ) and weak dephasing  $\gamma \sim 0$ , as seen in Fig. 1. In this case, the Fano factor reaches its maximum value at  $\mu_{\max}$  above the excited resonant level  $\varepsilon_2$ , and the transport is dominated by the two processes illustrated in Figs. 3(a) and 3(b), where an empty dot is occupied quickly, entering one of the two allowed states. Due to the weak coupling between the states, an electron is most likely to remain in the same state until it exits the dot. The entry rate is considerably faster than the exit rate, so one can ignore the time it takes an electron to enter the dot, and thus in both processes (a) and (b), the time intervals between entries are distributed exponentially. Most of the states in the lead at the energy  $\varepsilon_1$  are occupied, and therefore, an electron in the ground level has a lower exit rate than one in the excited state. Thus, the process is a combination of two exponentially distributed random processes, one of them faster than the other.

Within this picture, the time evolution of the dot's occupation is as follows: an empty dot is occupied immediately.

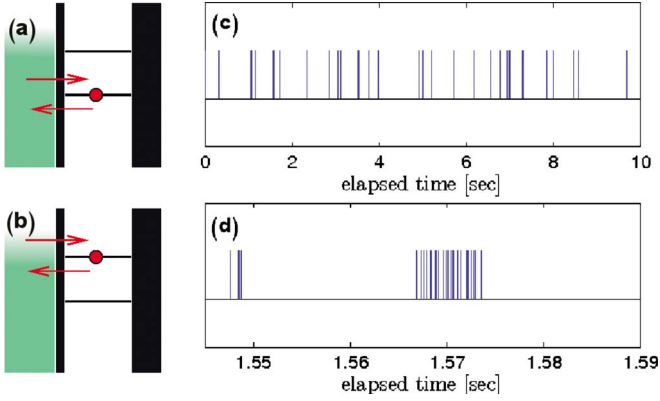


FIG. 3. (Color online) Transitions in a single-lead dot. (a) a “slow” process, involving the occupation of the ground level. (b) a “fast” process, involving the excited state. (c) and (d) present typical time traces, obtained from a numerical experiment, with parameters similar to those used in Fig. 2. In (c), the entire experiment is shown, where the stems represent entries of electrons into the dot. In the finer resolution (d), the fast processes can be seen.

If the electron enters the ground state, transport is blocked for the longer time scale  $1/\Gamma_{0\leftarrow 1}$  until the electron leaves the dot [process (a)]. If the excited state is entered, transport is blocked for a much shorter period [process (b)]. A series of such “fast” transitions would seem as a bunch of electrons tunneling into the dot and out of it at practically the same time.

Figure 3 presents typical results from a time-dependent simulation of the occupation of a two level dot, where the transition rates are as described above. Each time an electron enters the dot is registered as an “event” on the time-trace plotted in Figs. 3(c) and 3(d). These results demonstrate how events are clustered into groups of random size, which are separated by exponentially distributed time intervals of the longer time scale  $1/\Gamma_{0\leftarrow 1}$ . The individual fast events within a cluster are separated by the much shorter time scale  $1/\Gamma_{0\leftarrow 2}$ . Each cluster is terminated by an electron entering the ground state.

The resulting statistics display positive correlation between events, giving rise to a super-Poissonian distribution. Now the role of dephasing can be easily interpreted: inelastic scattering events bring about a finite probability for an excited dot to decay into the ground state, thus increasing the probability of terminating a cycle of fast events. As a result, the clusters become shorter and the correlation weaker. At high dephasing rates the transport is effectively governed by a single exponential process, just like the classical shot noise, resulting in a Poissonian distribution.

Following the above description, one looks at two transport channels with different “conductances,” one significantly larger than the other. It is possible to derive the full counting statistics of the transport process in this case, which leads to the Fano factor,

$$F = 1 + \frac{2p}{1-p}, \quad (6)$$

where  $p$  is the probability to tunnel through the open channel.<sup>15</sup> In a QD with a single contact and  $\Gamma_1 \ll \Gamma_2$ , the

open channel corresponds to the fastest countable process in Fig. 3(b), and its probability is given by

$$p = \frac{\Gamma_{2\leftarrow 0}}{\Gamma_{1\leftarrow 0} + \Gamma_{2\leftarrow 0}} \frac{\Gamma_{0\leftarrow 2}}{(\Gamma_{0\leftarrow 2} + \gamma)}. \quad (7)$$

Plugging this into the expression for the Fano factor [Eq. (6)], one arrives at Eq. (3). Note, however, that this reasoning can be applied at low temperatures and low dephasing rates only, where it is reasonable to assume exponentially distributed processes in both channels. When either temperature or dephasing are higher a sequence of several transitions could occur between two subsequent counts, such as  $|0\rangle \Rightarrow |2\rangle \rightarrow |1\rangle \rightarrow |0\rangle \Rightarrow |2\rangle$ , where only the two transitions marked by a double arrow are registered. The time intervals in this scenario have a much more complicated distribution.

## V. ENSEMBLE AVERAGING OF THE FANO FACTOR

In the previous sections, a dephasing-sensitive super-Poissonian noise peak was demonstrated for the two-level QD with a single contact, where particular parameters were used, such as  $\Gamma_1 \ll \Gamma_2$ , and temperature was low. In an attempt to attack the more general setup, we show here that this effect is significant not only in some specifically chosen systems but also for the ensemble averaged Fano factor. Within random matrix theory,<sup>17</sup> the tunneling rates are random variables with the Porter-Thomas distribution.

$$P(\Gamma) = \begin{cases} \frac{1}{\sqrt{2\pi\bar{\Gamma}}} e^{-\Gamma/2\bar{\Gamma}} & (\text{GOE}) \\ 1/\bar{\Gamma} e^{-\Gamma/\bar{\Gamma}} & (\text{GUE}), \end{cases} \quad (8)$$

where the tunneling rates through a given barrier average to the value  $\bar{\Gamma}$  regardless of energy. GOE stands for Gaussian orthogonal ensemble and GUE for Gaussian unitary ensemble.

The inelastic scattering rate between two states is proportional to the squared matrix element of the interaction  $V$ ,

$$\gamma_{ij} \propto |\langle i|V|j\rangle|^2, \quad (9)$$

where  $\psi_i = |i\rangle$  is an eigenstate of the dot’s Hamiltonian  $H_0$ . Whenever random-matrix theory is applicable, the spatial correlations of the electron wave function decay over a range of order of the Fermi wavelength  $\lambda_F$ ,<sup>17</sup> which is much smaller than the typical size of the dot ( $\lambda_F \ll L$ ). Assuming the interaction potential  $V$  varies slowly over a scale of  $\lambda_F$ , the integration in Eq. (9) can be approximated by a sum over small volume elements of linear size  $\lambda_F$ ,

$$\int_{\Omega} d\vec{r} V(\vec{r}) \psi_i^* \psi_j \sim \sum_{\Omega_k} V(\vec{r}_k) \psi_i^*(\vec{r}_k) \psi_j(\vec{r}_k). \quad (10)$$

where  $V(\vec{r}_k)$  is constant within each volume element  $\Omega_k$ . The wave functions are distributed randomly, and the dot’s linear size is typically much larger than  $\lambda_F$ . Therefore, the matrix element, given by the weighted sum of many product terms  $\psi_i^*(\vec{r}_k) \psi_j(\vec{r}_k)$ , is normally distributed. Accordingly, the dephasing rate  $\gamma$  is proportional to the square of this matrix

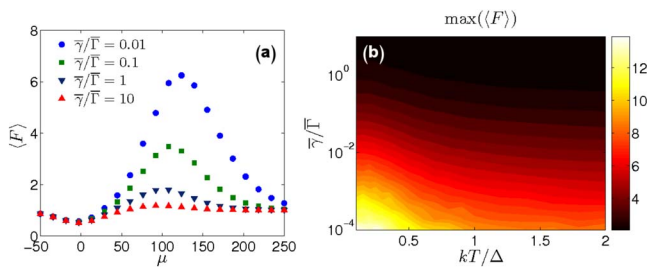


FIG. 4. (Color online) (a) The averaged Fano factor as a function of the leads' chemical potential at a low temperature. A peak in the noise to mean ratio is observed. Here,  $\varepsilon_1=0$ ,  $\varepsilon_2=100$ , and  $k_B T=20$  (arbitrary units). (b) The peak height for varying values of  $\bar{\gamma}/\bar{\Gamma}$  and  $kT/\Delta$ . Strong enhancement is observed when average dephasing rate is much lower than the average tunneling rate, and temperature is lower than the energy spacing. The Poisson value  $\langle F \rangle=1$  is reproduced for either large dephasing rate or high temperature.

element; hence, it is also distributed according to the Porter-Thomas distribution with an average value of  $\bar{\gamma}$ .

Figure 4 presents the results of the GUE ensemble averaging over  $\Gamma_1$ ,  $\Gamma_2$ , and  $\gamma$ . The averaged Fano factor is plotted as a function of the chemical potential and, similar to the particular cases discussed above, exhibits a clear peak. The dependence of the peak's height on  $\bar{\gamma}/\bar{\Gamma}$  and  $k_B T/\Delta$  is also

given. The peak height decreases with temperatures and dephasing rates, but should be clearly seen for  $k_B T \sim \Delta$  and low dephasing rates. Thus, the Fano factor seems to be a proper probe for observing the phase transition predicted in Ref. 1.

In summary, we study the peak in the Fano factor in the super-Poissonian regime and its dependence on the inelastic scattering rate and other relevant parameters. A convenient and simple analytical expression is developed for the peak location. Using experimentally relevant parameters, we estimate that the effect can be easily observed, as the average rate of events at the Fano factor peak ( $\mu \sim 140 \mu\text{eV}$ ) is of the order of 30 Hz [see Fig. 2(c)], where experiments of this kind were reported to last for as long as several minutes.<sup>18</sup> We thus propose to use the dephasing rate dependence as a probe for dephasing rates in closed quantum dots. This will enable measurements which are of great importance for any likely use of quantum dots as quantum computer memory units. The effect is still pronounced even after ensemble averaging. Further work is needed to extend the above analysis to the general multilevel dot.

#### ACKNOWLEDGMENTS

E.E. acknowledges support from an Alon fellowship at Tel-Aviv University.

- <sup>1</sup>B. L. Altshuler, Y. Gefen, A. Kamenev, and L. S. Levitov, Phys. Rev. Lett. **78**, 2803 (1997).
- <sup>2</sup>A. M. F. Rivas, E. R. Mucciolo, and A. Kamenev, Phys. Rev. B **65**, 155309 (2002).
- <sup>3</sup>U. Sivan, F. P. Milliken, K. Milkove, S. Rishton, Y. Lee, J. M. Hong, V. Boegli, D. Kern, and M. deFanza, Europhys. Lett. **25**, 605 (1994).
- <sup>4</sup>S. R. Patel, D. R. Stewart, C. M. Marcus, M. Gökçedağ, Y. Alhassid, A. D. Stone, C. I. Duruöz, and J. S. Harris, Phys. Rev. Lett. **81**, 5900 (1998).
- <sup>5</sup>J. A. Folk, C. M. Marcus, and J. S. Harris, Phys. Rev. Lett. **87**, 206802 (2001).
- <sup>6</sup>E. Eisenberg, K. Held, and B. L. Altshuler, Phys. Rev. Lett. **88**, 136801 (2002).
- <sup>7</sup>K. Held, E. Eisenberg, and B. L. Altshuler, Chaos, Solitons Fractals **16**, 417 (2003).
- <sup>8</sup>Y. M. Blanter and M. Büttiker, Phys. Rep. **336**, 1 (2003).
- <sup>9</sup>D. A. Bagrets and Y. V. Nazarov, Phys. Rev. B **67**, 085316 (2003).
- <sup>10</sup>B. R. Buřka, J. Martinek, G. Michałek, and J. Barnaś, Phys. Rev. B **60**, 12246 (1999); B. R. Buřka, *ibid.* **62**, 1186 (2000).
- <sup>11</sup>S. S. Safonov, A. K. Savchenko, D. A. Bagrets, O. N. Jouravlev, Y. V. Nazarov, E. H. Linfield, and D. A. Ritchie, Phys. Rev. Lett. **91**, 136801 (2003).
- <sup>12</sup>S. Gustavsson, R. Leturcq, B. Simovic, R. Schleser, P. Studerus, T. Ihn, K. Ensslin, D. C. Driscoll, and A. C. Gossard, Phys. Rev. B **74**, 195305 (2006).
- <sup>13</sup>A. Cottet and W. Belzig, Europhys. Lett. **66**, 405 (2004); A. Cottet, W. Belzig, and C. Bruder, Phys. Rev. Lett. **92**, 206801 (2004).
- <sup>14</sup>G. Kießlich, A. Wacker, and E. Schöll, Phys. Rev. B **68**, 125320 (2003).
- <sup>15</sup>W. Belzig, Phys. Rev. B **71**, 161301(R) (2005).
- <sup>16</sup>S. Gustavsson, R. Leturcq, B. Simovic, R. Schleser, T. Ihn, P. Studerus, K. Ensslin, D. C. Driscoll, and A. C. Gossard, Phys. Rev. Lett. **96**, 076605 (2006).
- <sup>17</sup>Y. Alhassid, Rev. Mod. Phys. **72**, 895 (2000).
- <sup>18</sup>S. Gustavsson, R. Leturcq, T. Ihn, K. Ensslin, M. Reinwald, and W. Wegscheider, Phys. Rev. B **75**, 075314 (2007).